ELSEVIER

Journal of Nuclear Materials 306 (2002) 218–231

journal of nuclear materials

www.elsevier.com/locate/jnucmat

Effect of helium on the swelling of GlidCop Al25 IG alloy

S.A. Fabritsiev [a,*], A.S. Pokrovsky [b], S.J. Zinkle [c], S.E. Ostrovsky [b]

[a] *D.V. Efremov Scientific Research Institute of Electrophysical Apparatus, Sovetsky pr.1, Metallostroy, 196641 St. Petersburg, Russia*

[b] *Scientific Research Institute of Atomic Reactors, 433510 Dimitrovgrad, Russia*

[c] *Oak Ridge National Laboratory, P.O. Box 2008, Oak Ridge, TN 37831-6376 USA*

Received 19 March 2002; accepted 5 October 2002

Abstract

This report presents data on the effect of neutron irradiation up to 0.5 dpa in the mixed spectrum SM-2 reactor at $T_{irr} \approx 160$ and ≈295 °C and on the TEM microstructure of GlidCop Al25 IG oxide dispersion strengthened copper after different heat treatments (CR + annealed, HIP). It is shown for the first time that a high helium generation rate in the alloy, due to boron introduced into the alloy in the capacity of deoxidizer, results in high-rate swelling of GlidCop Al25 IG of about 1%/dpa at 300 °C. It is shown that the average size of Al_2O_3 particles reduces under irradiation. The conclusion is made that the application of elements with high cross-sections of helium generation as deoxidizers can result in a substantial decrease of the resistance to swelling of copper alloys for fusion applications.

1. Introduction

Dispersion strengthened (DS) copper alloys containing ≈1 vol.% Al_2O_3 particles are considered as one of the most attractive materials for the ITER high heat flux components, like divertor and first wall [1].

The point of special importance for designers is that in the process of thermal treatment of the components at high temperature (800°–1000°) typical to brazing and hot isostatic pressing (HIP) reactions, alloys of DS type unlike precipitation hardened copper alloys (Cu–Cr–Zr, Cu–Ni–Be) retain their strengthening structure and high level of strength properties [2,3].

Even the first investigations of radiation stability of DS copper alloys showed their high resistance to radiation swelling. Up to irradiation doses of 16 and 63 dpa at 450 °C in the FTTF reactor [4,5] swelling of the GlidCop Al25 alloy was just 0.13% and 0.28%, respectively. Swelling of pure copper under the same conditions was 6.5% and 31% [4,5]. Irradiation to higher doses of 103 and 150 dpa at 415 °C in the FFTF did not result in swelling of the GlidCop Al25 alloy as well [6,7].

On the basis of these results, conclusions were made about the high resistance of DS copper alloys to swelling. However, all enumerated results were obtained at irradiation temperatures of 370–450 °C that substantially exceed the temperature where maximum swelling occurs in pure copper, i.e. ≈300 °C [8]. Moreover, all irradiations were performed in the fast reactors FFTF [4–7] and EBR-II [9] at a very low helium accumulation rate of 0.2 appm/dpa in pure copper and copper alloys without boron. At the same time the high accumulation rate of helium in copper of 10 appm/dpa is typical for fusion reactors [1]. Hence, the obtained estimates of DS copper alloy resistance to swelling are highly uncertain when compared with anticipated fusion operation conditions. The fact that the high helium accumulation rate can in principle influence the DS copper alloy swelling was shown in the study [10]. In case of GlidCop Al60 irradiation by heavy ions at 350 °C, simultaneous helium implantation at the rate of 30 appm/dpa augmented the swelling rate of alloy from 0.01%/dpa to 0.05%/dpa. In general it should be pointed out that up to now no data have been obtained on the influence of the high helium

* Corresponding author. Tel.: +7-812 464 4463; fax: +7-812 464 4623.

E-mail address: fabrsa@sintez.niiefa.spb.su (S.A. Fabritsiev).

0022-3115/02/$ - see front matter
PII: S0022-3115(02)01310-7

accumulation rate on swelling of DS copper alloys under neutron irradiation at temperatures near to the swelling maximum.

This study presents the first results of such investigation carried out for the GlidCop Al25 IG alloy at an irradiation temperature of 295 °C and high helium accumulation rate.

2. Experimental procedure

Materials for the investigation were DS copper alloys GlidCop Al25 IG (OMG, US) and MAGT 0.2 (GIPROCMO, RF). Aimed to produce an improved modification of GlidCop Al25 alloy the OMG Company has developed a procedure providing the higher plasticity of the new GlidCop Al25 IGO modification retaining a sufficiently high level of the strength and thermal conductivity [11]. The first investigations of this material showed good properties in the unirradiated state [11]. The GlidCop Al25 IG alloy contained 165 ppm boron in the capacity of deoxidizer. Three groups of GlidCop Al25 IG alloys were investigated in the study:

(a) GlidCop Al25 IG (CR + ann) specimens were cut from a plate fabricated by hot extruding, then the plate was cross-rolled (CR) and annealed in order to homogenize it at 900 °C for 1 h. Specimens were cut from the plate in the transverse direction to extrusion. GlidCop Al25 IG (CR + ann) manufacturing is described in [12].
(b) Specimens of GlidCop Al25 IG HIP JA were cut from the copper part of the joint GlidCop Al25 IG/316LN (JA), manufactured by HIP. During the HIP treatment at the last fabrication stage, the joint underwent heating at 1020 °C. Specimens from the copper part of the joint were also cut in the transverse direction. Details of the GlidCop Al25 IG HIP JA alloy manufacturing are shown in [13].
(c) Specimens of GlidCop Al25 IG HIP EU were cut from the copper part of the GlidCop Al25 IG/316LN (EU) joint manufactured by hot pressing. During the HIP treatment at the last stage of joint fabrication underwent heating at 980 °C. Specimens from the copper part were also cut in the transverse direction. Details of the GlidCop Al25 IG HIP EU manufacturing are shown in [14].

The MAGT 0.2 alloy has a technological history very similar to the procedure of the GlidCop Al25 IG HIP EU alloy manufacturing. It was also extruded, and then the sample was stuck by HIP at 980 °C to the plate of 316LN steel [15]. However, the alloy contained deoxidizing admixtures of Hf and Ti. As can be seen in Table 1 the boron content in this alloy was low, about 0.5 ppm.

Flat specimens (1 mm thick) of STS type with the gauge length of 10 mm were cut from the alloy samples. Specimens were irradiated in the SM-2 reactor in two irradiation facilities (SPP-1 and SPP-3) in sealed capsules filled with helium.

The specimens were irradiated in the SPP-1 irradiation facility to the maximum fast neutron fluence $\Phi t_{\text{fast}} = 8.5 \times 10^{24}$ n/m^2 ($E > 0.1$ MeV) at (160 ± 10) °C and the SPP-3 irradiation facility to $\Phi t_{\text{fast}} = 9.1 \times 10^{24}$ n/m^2 ($E > 0.1$ MeV) at (295 ± 15) °C that corresponds to damage doses of 0.58 and 0.62 dpa, respectively (fast neutron flux $\approx 5.3 \times 10^{18}$ n/m^2 s). The maximum thermal neutron fluence with the energy $E < 0.67$ eV was $\Phi t_{\text{therm}} = 11.5 \times 10^{24}$ n/m^2 for SPP-1 and $\Phi t_{\text{therm}} = 12.3 \times 10^{24}$ n/m^2 for SPP-3. Calculations of the accumulated helium content in specimens carried out according to the procedure in [16] predict (Table 2) that specimens of GlidCop Al25 IG accumulated about 195 appm He whereas the MAGT 0.2 alloy generated 0.5 appm He.

Irradiation of GlidCop Al25 and MAGT0.2 alloys, which are similar in composition and structure, to the same damage dose under equivalent irradiation conditions allowed an assessment to be made of the influence of helium accumulation on radiation damage of DS copper alloys. Specimens (unirradiated and irradiated) were tested in tension at $T_{\text{test}} = T_{\text{irr}}$ at a deformation rate of 1.66×10^{-3} s^{-1}. Testing was carried out in vacuum at 10^{-4} Pa.

TEM investigations were performed using the JEOL 2000FX electron microscope at an accelerating voltage of 120 keV. TEM discs of 3 mm diameter were cut from the gauge length of tested specimens and from non-deformed areas as well. Cut samples were mechanically thinned to 0.3 mm and then TEM specimens were prepared using an electro-chemical procedure.

Void photographs were obtained using kinematic low contrast conditions and slight under-focusing. We used weak – beam dark field imaging for alumina particle

Table 1
Alloy composition (wt%)

Material	Cu	Al[a]	B	Fe	Pb	Ti	Hf
MAGT0.2	Bal.	0.24	0.00005	0.017	–	0.14	0.03
GlidCop Al25 IG	Bal.	0.25	0.0165	0.0048	0.0008	–	–

[a] as Al_2O_3.

Table 2
Irradiation conditions

Material	T_{irr} (°C)	$\Phi t_{fast} \times 10^{24}$ (n/m^2), $E > 0.1$ (MeV)	$\Phi t_{therm} \times 10^{24}$ (n/m^2), $E < 0.67$ (eV)	Average damage (dpa)	Maximum helium concentration (appm)
GlidCop Al25 IG	160	7.5–8.5	7.5–11.5	≈0.5	≈195
	295	7.1–8.6	9.6–11.6	≈0.5	≈195
MAGT0.2	295	8.8–9.1	11.6–12.3	≈0.5	≈0.5

diameter measurements. Approximately 1500 clusters from different foils were counted for every irradiation condition of the material. The foil thickness was measured using convergent beam electron diffraction with the direction parallel to [2 2 0] Cu.

3. Results

Metallographic investigations of the GlidCop Al25 IG alloy showed that it has a structure practically equiaxial along longitudinal and transverse directions and highly (1/5) elongated across the short transverse direction (crosswise the plate thickness). A typical TEM microstructure of the alloy specimen consisting of equiaxial grains of 0.5–2 μm is shown in Fig. 1(a). The Al_2O_3 particles have dimensions of 4–25 nm and high density 1.2×10^{22} m^{-3}. The distribution of Al_2O_3 particles in the grain structure was highly heterogeneous. The analysis of reflections obtained from the particles in dark field image (Fig. 1(b)) shows that their structure corresponds to the lattice parameter of 0.802 nm that allows to identify them as η'-Al_2O_3 described by Ernst et al. [17]. Moiré fringes were observed in some areas of particles that have the form of triangular shaped platelets.

The dislocation density in unirradiated non-deformed specimens is less than 10^{14} m^{-2} since for all three states of the GlidCop Al25 IG alloy the latest thermal treatment was an annealing at 980–1020 °C. The TEM analysis of unirradiated specimens cut from three different batches of the GlidCop Al25 IG alloy (a, b, c) did not show remarkable details in the alloy structure, dimension and density of Al_2O_3 particles, that look obvious because in the process of joint fabrication (JA and EU) typical GlidCop Al25 IG (low oxidation – LOX materials) plates with similar chemical composition were used.

The size distribution of Al_2O_3 particles (Fig. 2(a)) shows a maximum in the range of 4–7 nm and extends up to 24 nm. If we compare our average size of Al_2O_3 particles in GlidCop Al25 alloys with other results [18–22] for the same material, good coincidence can be pointed out (Table 3). Whereas the maximum distribution falls in the range 8–10 nm, the mean size of particles is close to that determined by us and equals in about 7 nm. Though it is not specified in the studies [18,20,21] GlidCop Al25 apparently without boron is discussed and moreover in the as-extruded state. In general the mode of size distributions is similar. In all cases distributions have a remarkable tail towards the range of large size particles.

The investigation of the TEM structure of specimens tested at 150 and 300 °C showed that Al_2O_3 particles are an efficient barrier for the deformation development. Bending of dislocations around particles was observed, however, in general the deformation of unirradiated specimens develops intensively that corresponds to sufficiently high plasticity characteristics of unirradiated alloys.

3.1. Irradiation at 160 °C

In specimens irradiated at 160 °C (CR + ann, and also HIP JA), a high density of small defects clusters was observed (Fig. 1(c)). The defect cluster density was about 7×10^{22} m^{-3} and the average size of defects about 1.35 nm. The main type of these defects in copper are stacking fault tetrahedra (SFT) at these temperatures and irradiation doses [18,23–25].

Table 4 shows the measurement results of density and size of defect clusters and Al_2O_3 particles. The density of Al_2O_3 slightly increases under irradiation but remains in the range of measurement scattering $(1.24 \pm 0.16) \times 10^{22}$ m^{-3} for unirradiated and $(1.66 \pm 0.35) \times 10^{22}$ m^{-3} for irradiated specimens.

Histograms with size distributions of Al_2O_3 particles before and after irradiation (Fig. 2(b)) were made on the basis of TEM images. The irradiation obviously leads to a shift of the size distribution towards lower values. The average size of particles under irradiation decreases to (4.74 ± 0.75) nm as compared with (6.54 ± 0.52) nm in the unirradiated state, and this decrease goes off the scattering range. The same effect was observed in a number of other experiments both under neutron [7,18] and ion irradiations [20,26].

The investigation of the structure of specimens irradiated and deformed at 150 °C shows that dislocations are efficiently hampered by both SFT and Al_2O_3 particles. Dislocation pinning and hang-up are observed in

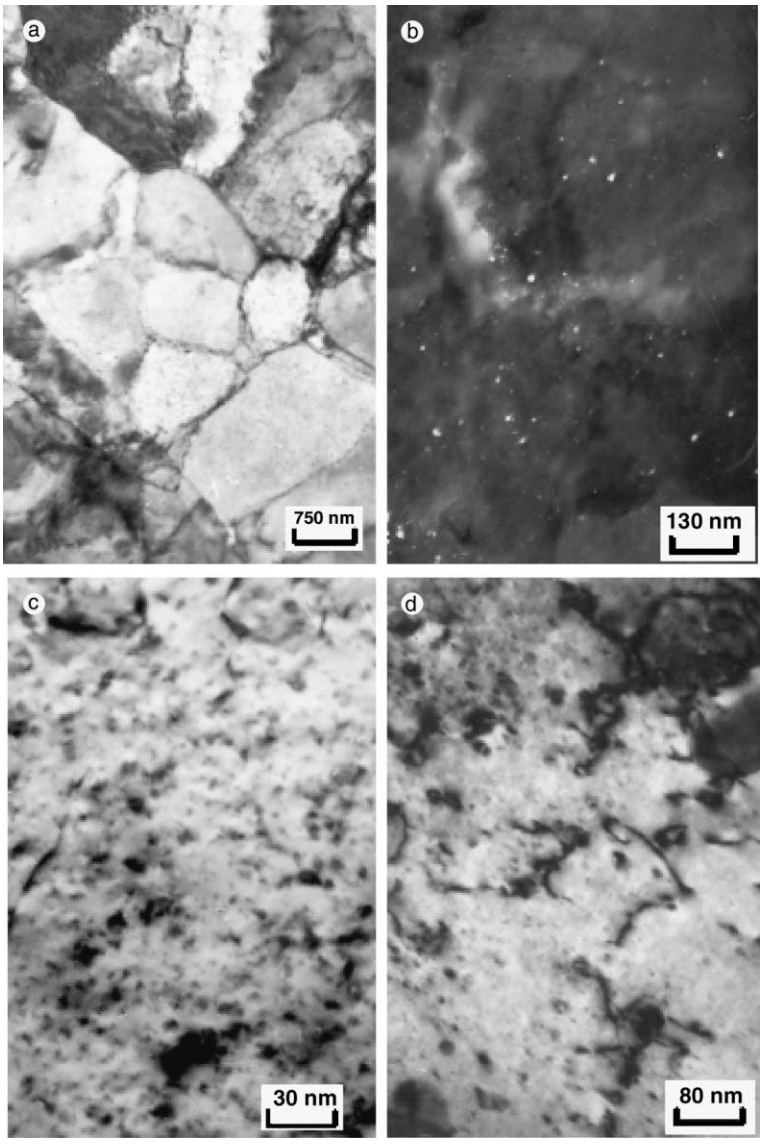

Fig. 1. TEM structure of GlidCop Al25 IG (CR + annealed) alloy: (a) unirradiated condition, general view; (b) Al_2O_3 particles, dark field; (c) 0.57 dpa, $T_{irr} = 160$ °C, as irradiated condition; (d) irradiated and tensile tested.

many regions (Fig. 1(d)). The picture like channelling is rarely observed that nevertheless can be explained as channelling and possibly takes place in general in the area of maximum stresses, i.e. in the specimen region where local deformation and subsequent failures have occurred. It is clear that TEM specimens were manufactured of regions to be at the distance from the failure area not less than 1.5 mm and therefore can be evidence of only the mode of uniform deformation development in specimens which is low for irradiated specimens, just 0.8% compared 5.8% in case of unirradiated specimens. In fact resolvable dislocation loops were not observed in specimens, whereas they are observed in pure Cu irradiated at 210 °C [25].

3.2. Irradiation at 300 °C

Irradiation to 0.5 dpa at 300 °C results in the pronounced void formation (Figs. 3(a)–(d)) and appearance of small helium bubbles (Figs. 4(a) and (b)) in the GlidCop Al25 IG.

A very small density of defect clusters was observed in specimens irradiated at 300 °C. The main

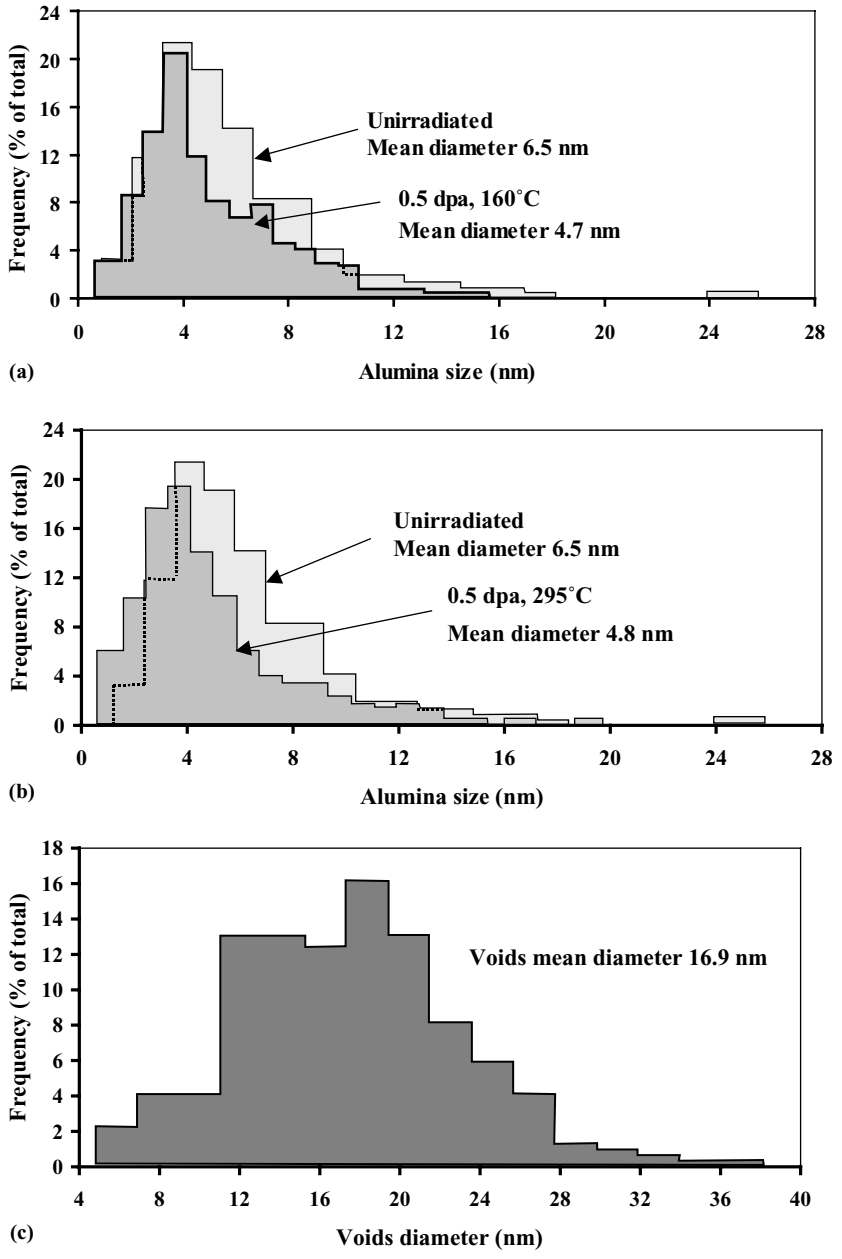

Fig. 2. The effect of neutron irradiation to 0.5 dpa at (a) 160 °C and (b) 295 °C on the Al_2O_3 particle size distribution in GlidCop Al25 IG alloy; (c) the effect of neutron irradiation to 0.5 dpa at 295 °C on the size distribution of voids in GlidCop Al25 IG alloy.

element of the microstructure were vacancy pores whose average size was (16.9 ± 2.0) nm and density (1.07×10^{21}) m^{-3} that corresponds to the average swelling of $(0.5 \pm 0.2)\%$. The crystallographic analysis showed that the pores had surface facets corresponding to {1 1 1} planes of the Cu alloy matrix (Fig. 3(b)). For example in pure Cu irradiated to 1.1 dpa at 300 °C [8] vacancy pores have a mean diameter 45 nm and density 6.5×10^{19} m^{-3}.

The void denuded zone along the grain boundaries (Fig. 3(a)) had the width of 65 nm and was 10 times narrower as compared with the zone in pure copper irradiated by neutrons at 350 °C [8]. The dimension of the void denuded zone is comparable with the average distance between pores.

Histograms of the void size distributions (Fig. 2(c)) show the obvious maximum in the range of 12–

Table 3
Alumina particle size and density in unirradiated conditions

No.	Materials	Specimens	Reference	Conditions	
				Al_2O_3 density (10^{22} m^{-3})	Al_2O_3 mean diameter (nm)
	GlidCop A125 IG, 165 ppm B				
1	(CR + ann)	RF11	This work	1.2	6.25
2	(CR + ann)	RF12	This work	0.88	7.3
3	(CR + ann)	RF13	This work	1.4	5.83
4	From HIP JA Joints	JA21	This work	1.6	6.56
5	From HIP JA Joints	JA22	This work	1.3	6.04
6	From HIP JA Joints	JA23	This work	1.27	7.59
7	From HIP JA Joints	JA24	This work	1.22	6.93
8	From HIP EU Joints	EU31	This work	1.16	6.75
9	From HIP EU Joints	EU32	This work	1.39	5.43
10	From HIP EU Joints	EU33	This work	0.94	6.73
	Average unirradiated 1–10			1.24 ± 0.1 6	6.54 ± 0.52
11	GlidCop A125 extruded, no B,		[18]	2.2	8.7
12	GlidCop A115, 50% c.w. + 200 ppm B, Extruded		[19]	3	5
13	GlidCop A125, + 200 ppm B, aged		[19]	2.2	6.2
14	GlidCop A120, c.w. + 200 ppm B		[19]	4.7	3.3
15	GlidCap A125, extruded, no B		[20]	4.5	8
16	GlidCop A125, extruded, no B		[21]	3	7
	Average unirradiated 11–16			3.27 ± 0.89	6.37 ± 1.53

Table 4
Effect of neutron irradiation at 160 °C on defect clusters and Al_2O_3 particle size and density

Materials	Specimens	Conditions						
		TEM image (#)	Dose (dpa)	T_{irr} (°C)	Al_2O_3 density (10^{22} m^{-3})	Al_2O_3 mean diameter (nm)	Defect cluster density (10^{22} m^{-3})	Defect cluster mean diameter (nm)
GlidCop A125 IG, 165 ppm B								
From HIP joints, JA	2P059	1788	0.57	160	1.67	5.94	6.8	1.31
From HIP joints, JA	2P059	1784	0.57	160	1.84	4.18	6.5	1.27
From HIP joints, JA	2P059	1785	0.57	160	1.57	5.65	5	1.4
From HIP joints, JA	2P059	1782	0.57	160	1.2	4.87		
CR + ann	1P001	1777	0.43	160	1.15	3.37	9.46	1.4
From HIP joints, EU	2P054	1794	0.59	160	2.5	4.42		
Average					1.66 ± 0.35	4.74 ± 0.75	6.94 ± 1.26	1.35 ± 0.05

20 nm. However, some pores are larger – up to 35 nm – and comparable with pore dimensions in pure copper [8].

The second component of the structure are small helium bubbles, $d \approx 1.13$ nm, whose density is very high, $\simeq 6.4 \times 10^{23}$ m^{-3} (Figs. 4(a) and (b)). The bubbles are resolved only in thin foil areas and observed both in the grain interior and on grain boundaries. An increase of the size of helium bubbles on grain boundaries was not observed.

The optimum contrast of pores and Al_2O_3 inclusions is obtained under different conditions and therefore two images with different focusing were made on many areas, in one case in order to obtain the optimum contrast of voids (Fig. 3(c)), in the other case the optimum contrast of Al_2O_3 particles (Fig. 3(d)) in the same area. As

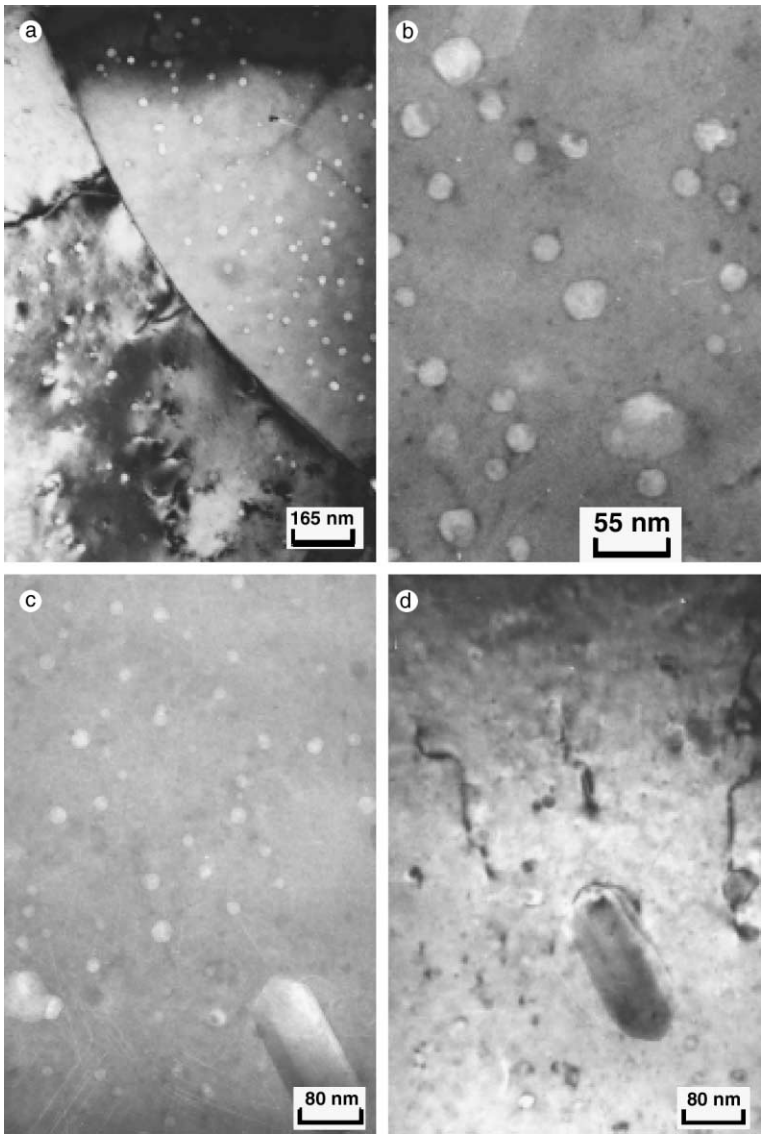

Fig. 3. (a–d) TEM structure of GlidCop Al25 IG (CR + annealed) alloy, ≃0.5 dpa, $T_{irr} = 295$ °C, as-irradiated condition, voids in structure.

follows from Fig. 3(d) in some cases, the association of voids and relatively large Al_2O_3 particles of about 10 nm in diameter are observed. Many voids are bounded by dislocations. As follows from Table 5, voids are observed in all three investigated modifications of GlidCop Al25 in CR + ann and solid HIP states.

The analysis of Al_2O_3 particle size distribution for specimens irradiated at 300 °C shows that all the three grades of GlidCop Al25 exhibited a reduction of the average size of Al_2O_3 particles (Table 5). The histogram of the Al_2O_3 particle size distribution (Fig. 2(b)) shows that the average size of Al_2O_3 particles after 160 and 300 °C irradiation reduces from 6.5 to (4.8 ± 0.8) nm, i.e. the value is out of the scattering range. The density of Al_2O_3 particles is within the scattering range measured for the unirradiated alloy. TEM investigations of the specimens cut from the gauge length of specimens tested at 300 °C showed that the material undergoes an intensive process of recovery and formation of the dislocation cell structure when deforming by the higher test temperature as compared with 150 °C. Dislocation networks as seen in Fig. 3(d) are pinned by both Al_2O_3 particles and voids. However, due to dislocation climb and glide, the deformation goes easier than at the test temperature

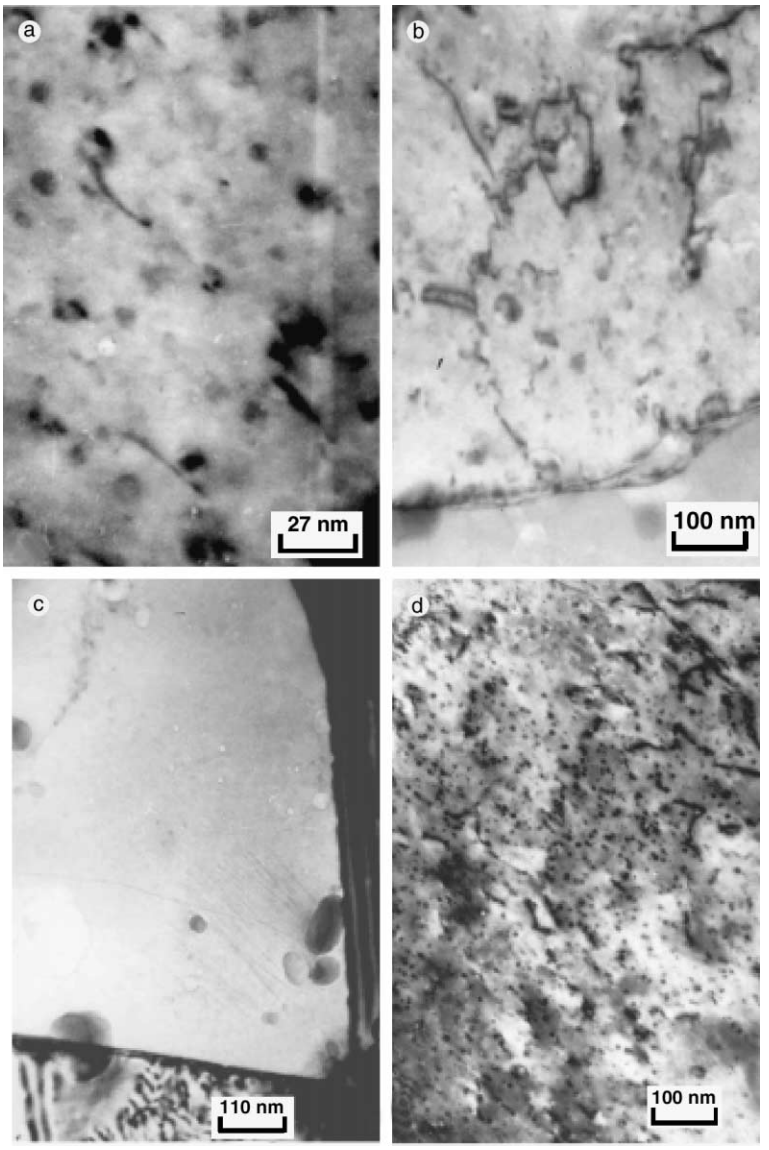

Fig. 4. TEM structure of GlidCop Al25 IG (solid HIP from JA joints) and MAGT0.2 alloys: (a) 0.56 dpa, $T_{irr} = 295$ °C, as-irradiated condition, He bubbles in structure; (b) 0.56 dpa, $T_{test} = 300$ °C, $T_{irr} = 295$ °C, irradiated and tensile tested, dislocation creep; (c) 0.5 dpa, $T_{irr} = 295$ °C, annealed at 900 °C, 1h; (d) MAGT0.2 (extruded and solid HIP) alloy, irradiated to 0.54 dpa at $T_{irr} = 295$ °C.

150 °C. This corresponds to the fact that the specimens have a relatively high uniform elongation of about 8% at $T_{test} = T_{irr} = 300$ °C.

3.3. Effect of annealing at 900 °C on the structure of the GlidCop Al25 IG alloy

Some specimens were annealed at 900 °C for 1 h after irradiation at 300 °C. As was previously mentioned, this annealing in the unirradiated state (HIP specimens) did not significantly change either the density or the size of Al_2O_3 particles, and did not affect the mechanical properties of the unirradiated alloy.

As follows from Fig. 4(c) vacancy voids disappear completely after annealing. Helium bubbles still remain. Their size significantly increases from ≈1.3 nm in the as-irradiated condition to 15 nm after the 900 °C anneal. The helium bubble density is much lower than that for non-annealed specimens irradiated at 300 °C. Helium bubbles are observed both in the grain interior, where they are bound with dislocations, and on grain boundaries (Fig. 4(c)). Some bubbles have a size up to 60 nm. Faceted surfaces on helium bubbles are not observed.

Table 5
Effect of neutron irradiation at 295 °C on voids, helium bubbles and Al_2O_3 particles size and density

Materials	Specimens	Conditions									
		TEM image (#)	Dose (dpa)	T_{irr} (°C)	Al_2O_3 density (10^{22} m^{-3})	Al_2O_3 mean diameter (nm)	Voids density (10^{21} m^{-3})	Voids mean diameter (nm)	Swelling (%)	He bubbles density (10^{23} m^{-3})	He bubbles mean diameter (nm)
GlidCop A125 IG, 165 ppm B											
From HIP joints, JA	3P099	1705	0.56	295						5.4	1.13
From HIP joints, JA	3P099	695	0.56	295			1.04	19.65	0.57		
From HIP joints, JA	3P099	690	0.56	295			0.85	16.9	0.26		1.8
From HIP joints, JA	3P099	689	0.56	295			0.57	17.9	0.39		
From HIP joints, JA	3P099	693	0.56	295			1.58	16.44	0.44		1.13
From HIP joints, JA	3P099	1700	0.56	295			1.08	18.2	0.84		
From HIP joints, JA	3P099	1703	0.56	295			0.83	21.2	0.91		
From HIP joints, JA	3P099	1704	0.56	295			0.87	13.15	0.268		
From HIP joints, EU	3P115	1829	0.5	295			1.7	12.87	0.22		
CR + ann	3P063	1813	0.41	295			1.05	14.91	0.49		
CR + ann	3P063	1812	0.41	295			1.17	17.3	0.7		
From HIP joints, JA	3P099	1688	0.56	295	1.53	5.43	0.3	12.96	0.11		
From HIP joints, JA	3P099	1686	0.56	295	2.1	4.17					
From HIP joints, JA	3P099	694	0.56	295	1.6	4.78					
From HIP joints, EU	3P115	1836	0.5	295	1.46	6.75				7.46	1.18
CR + ann	3P063	1814	0.41	295	1.86	4.03					
CR + ann	3P063	1816	0.41	295	0.73	3.9					
Average					1.55 ± 0.31	4.84 ± 0.83	1.07 ± 0.25	16.85 ± 2.01	0.51 ± 0.20	6.43 ± 1.03	1.31 ± 0.25

The density and size of Al_2O_3 particles in annealed specimens were not measured but from the qualitative point of view they are similar to those of non-annealed irradiated specimens.

3.4. Structure of the MAGT0.2 alloy irradiated at 300 °C to 0.5 dpa

The structure of the MAGT0.2 boron-free alloy that is relatively free of helium after irradiation at 300 °C differs from the structure of GlidCop Al25 IG. There were no voids or helium bubbles (Fig. 4(d)). The TEM analysis of the defect structure showed that defect clusters and loops are predominant.

Thus, at the same irradiation dose two DS alloys fabricated according to the same procedure and containing close amounts (about 0.25%) of Al_2O_3 show completely different resistance to vacancy swelling. The GlidCop Al25 IG alloy has swelling of 0.5%; the MAGT0.2 alloy has no observable cavities.

4. Discussion

Main irradiation effects found in this study are primordial high swelling of the GlidCop Al25 IG alloy at 0.5 dpa at 300 °C and recoil resolution of Al_2O_3 particles at 0.5 dpa at irradiation temperatures of 160 and 300°. Let us consider separately each effect.

4.1. Swelling of the GlidCop Al25 IG0 alloy

One of the main advantages of DS alloys, which are a reason for their inclusion into the fusion program, was a very high resistance to radiation swelling found in the first studies [4,5]. However, these data correspond to the irradiation temperature of 400–450 °C, meanwhile the temperature maximum of swelling for copper is ≈300 °C [8]. It should be pointed out that regardless of a very large number (>100 studies) of publications on the radiation stability of DS copper alloys the real temperature dependence of swelling under neutron irradiation in the range of 220–350° was not obtained. Thus, in our consideration we have to be grounded on the maximum swelling point of pure copper at ≈300 °C [8].

The analysis of publications shows that, though GlidCop Al25 and GlidCop Al60 alloys up to 150 dpa did not reveal swelling at irradiation in FFTF, there is a number of studies to be evidence of some unclear points. Spitznagel et al. [10] showed that the GlidCop Al60 alloy when co-implanting helium at the rate of 30 appm He/dpa swells much faster than without helium, to 0.8% at 20 dpa. Edwards et al. [27] reported that after irradiation in the FFTF at 415 °C to 103 dpa the alloys GlidCop Al20, GlidCop Al25 practically did not swell while the GlidCop Al15 + B alloy swelled by 11%. Garner et al. [28] showed that the GlidCop Al25 alloy irradiated to 98 dpa at 450 °C swelled by about 2%.

On the other hand, the investigation of the MAGT0.2 alloy irradiated to 7 dpa in BOR-60 at lower temperature of about 345 °C did not reveal swelling [29]. Frost and Kennedy [30] showed earlier that the irradiation of alloys GlidCop Al20 and Al60 in EBR-II at 385 °C to 10 dpa practically had not changed their density ($S < 1\%$). We should point out in all these irradiations, that the alloys MAGT0.2 and GlidCop were used in the as-extruded or as-extruded +20–50% cold working states, i.e. materials with a very high dislocation density ($\approx 5 \times 10^{15}$ 1/m^2) [20]. The boron content in these alloys did not exceed 0.2–1 ppm [31]. Data on swelling of GlidCop Al25 IG containing about 150–200 ppm boron in the capacity of deoxidizer in the CR + ann state, i.e. after annealing at 900 °C for 1 h (at low dislocation density) are lacking in previous studies.

Since the study obviously established the difference in tendencies of both DS alloys irradiated under the same conditions to swelling let us consider the differences of these alloys in detail. Ti and Hf were introduced into the MAGT0.2 alloy as deoxidizers but boron was not. The size of Al_2O_3 particles in this alloy is somewhat larger than that in GlidCop Al25 IG, and the density of particles is somewhat lower [22]. Both the alloys are manufactured by a similar procedure that includes powder manufacturing, internal oxidation of the powder and powder compacting by the HIP procedure. After that the GlidCop Al25 IG samples are extruded, cross-rolled and then annealed at 900 °C for 1 h.

The MAGT0.2 alloy was extruded and then HIPped for the MAGT0.2/316LN joint. The HIP procedure at 980 °C for 1 h was the last thermal treatment of the MAGT0.2 alloy. Therefore, the dislocation density in both the alloys is rather low. Hence, it is difficult to simply attribute the higher swelling of GlidCop IG to the lack of the cold deformation and low dislocation density.

The difference between MAGT0.2 and GlidCop IG is that boron was introduced as deoxidizer, and Ti and Hf were used for this purpose in MAGT0.2. As a result, the amount of accumulated helium in the MAGT0.2 alloy was about 0.5 appm after irradiation to 0.5 dpa, and about 195 appm in the GlidCop IG alloy, completely due to the transmutation of ^{10}B.

The influence of boron additions on swelling is sufficiently well studied for pure copper. In particular the study [32] shows that the boron addition and high helium generation rate controlled by boron under neutron irradiation at 250 and 350 °C (107 appm He at 1.2 dpa) produce helium bubbles. The values of swelling in pure copper and in the Cu–B alloy are similar but the size of cavities in the latter is significantly (as much as 1.5 times) higher than in the boron-free alloy [8,32,33].

The lack of a typical halo around the boride particles in the irradiated GlidCop Al25 IG as it was observed in many studies in the Cu–B system [34,35] proves that boron was uniformly dispersed into the GlidCop Al25 IG alloy and therefore the helium content and its generation are uniformly distributed throughout the specimen bulk.

The analysis of the observed GlidCop Al25 IG alloy structure after irradiation allows the following way of vacancy porosity development under irradiation. Since the alloy contains high-density Al_2O_3 particles of which the surface plays the role of efficient sinks during initial stages of irradiation (dose of about 0.05 dpa $c_{He} \approx 30$ appm), efficient recombination of radiation defects takes place in these sinks. However, helium accumulates in the alloy precipitates on dislocations, grain boundaries and interfacial areas of Cu/Al_2O_3.

As a result, when the dose reaches 0.1 dpa and the helium content 60 appm, the system of dislocations fixed in nodes by helium bubbles is created in the matrix which possesses the strong preference to absorb interstitials. As a result, vacancies form complexes which can turn into voids. Helium can stabilize the nucleation of small cavities; sometimes helium bubbles on Al_2O_3 particles work as void embryos. Voids contain some helium but mainly they are formed by vacancies. Due to this reason they are efficiently annealed at 900 °C.

According to this picture the high helium accumulation rate stimulates swelling of GlidCop IG in two ways:

- Helium accumulation, happens by means of stopping the dislocations and creating the system with stable sinks that preferentially absorb interstitials (this mechanism occurs in austenitic steels only at 5–10 dpa [36]).
- Helium stabilizes small pores.

In the MAGT0.2 alloy where helium is practically not generated both the mechanisms are not implemented and therefore vacancy voids do not arise. This also explains the lack of significant cavity swelling in GlidCop Al25 irradiated with ions up to high doses [10,22,26].

What about outlooks of the GlidCop Al25 IG alloy in real fusion application from the point of view of its tendency to swelling? Copper accumulates about 10 appm/dpa due to the hard fusion neutron spectrum in the alloy [1]. In other words at 1 dpa the alloy will contain about 10 appm He due to threshold reactions on ^{63}Cu and ^{65}Cu. It also should be taken into account that the fusion reactor is a large device consisting of high amounts of metals and therefore neutrons will be moderated. If we qualitatively assess the thermal constituent of the full neutron spectrum as much as 0.05, then not less than 30 appm He will be accumulated in ^{10}B at 1 dpa. Altogether under fusion conditions the accumulation rate on GlidCop IG0 could be about 40 appm/dpa for ≈1dpa exposure.

In our experiment the rate of accumulation was substantially higher, about 300 appm/dpa, but it should be pointed out that the stabilization of helium on dislocation nets in fcc metals is implemented at helium concentrations of about 50–100 appm [37]. Therefore, there is an apprehension that the tendency to early and high-intensive (at the rate of about 1%/dpa) swelling should be typical for DS alloys in the case of irradiation in fusion reactors where boron is used as a deoxidizer. Hence, the use of Hf and Ti, which are stable enough under irradiation in the capacity of deoxidizers, is a more promising approach from the point of view of nuclear application.

Fig. 5(a) shows assembled neutron irradiation data on the copper DS alloy swelling with and without boron. The data suggest that the helium generation results in a significant increase of the swelling rate of the GlidCop alloy when irradiated in both the mixed spectrum reactor SM-2 and fast reactor FFTF [4,27–29].

4.2. Changes in dimensions of Al_2O_3 particles under irradiation

The observations in this study regarding the radiation-induced decrease of the average Al_2O_3 particle size agree with results of other studies where the stability of Al_2O_3 under neutron or ion irradiation was investigated [7,10,20,22,26]. In all studies where the size distribution of Al_2O_3 particles was measured, a increment of the average particle size was observed.

The observed effect found for the first time in 1986 was explained by processes of recoil resolution of Al_2O_3 under irradiation [38,39]. However, in our case this explanation looks forced since recoil resolution processes can significantly reduce the size of Al_2O_3 particles only at doses above about 20 dpa [38]. We consider only 0.5 dpa.

Let us consider other explanations of the fact besides changes in size. From our point of view great support comes from the measurement results of yield strength of unirradiated, irradiated, and irradiated and annealed specimens of the GlidCop Al25 IG alloy (Fig. 5(b)). Annealing at 900–980 °C practically does not change the yield strength properties of GlidCop IG in the unirradiated state. Therefore, we do not see any difference in yield strength of GlidCop Al25 IG (CR + ann) and GlidCop Al25 IG in the solid HIP condition. A clear tendency is observed at the same time after irradiation at 300 °C: the yield strength of alloys irradiated and annealed at 900 °C for 1 h is lower by 30–40 MPa as compared with unirradiated specimens (the yield strength reduction after annealing significantly exceeds scattering of about 15 MPa). Since the high yield strength of GlidCop is controlled by Al_2O_3 particles,

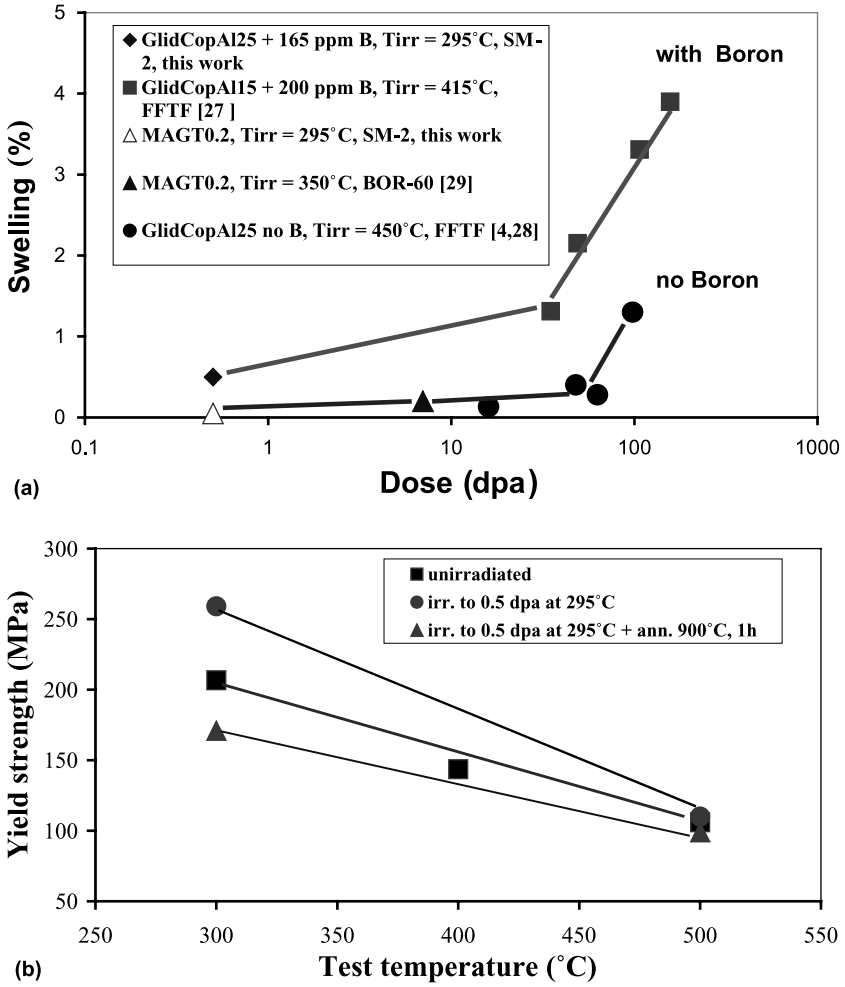

Fig. 5. (a) Boron effect on swelling of GlidCop copper alloys, irradiated in the mixed spectrum SM-2 reactor and fast neutron reactors BOR-60 and FFTF between 295 and 450 °C; (b) the effect of annealing at 900 °C, 1 h on the yield strength of neutron-irradiated GlidCop Al25 IG (CR + ann) copper alloy (0.5 dpa at $T_{irr} = 295$ °C).

which are efficient barriers for dislocations it is possible to conclude that the reduction of yield strength is also a factor indirectly confirming the real reduction of the number of barriers (density of Al_2O_3) as a result of irradiation to 0.5 dpa. A reason of the decrease of the average Al_2O_3 particle size at so low dose of 0.5 dpa are possibly additional sources of damage due to recoil ions.

According to the philosophy developed in Ref. [40] passing of ions through the Al_2O_3 particles causes additional (beyond the primary damage by neutrons) radiation damage of Al_2O_3. The reaction of helium accumulation is ^{10}B (n,α) ^{7}Li, where the ^{4}He ion has an energy of 1.47 MeV, and the ^{7}Li ion an energy corresponding to 0.84 MeV. The range of $^{4}He + {}^{7}Li$ ions in copper are 2.6 and 1.3 μm, respectively, thus, comparable with the grain size of GlidCop Al25 IG. However, the calculation of additional radiation damage by ion irradiation gives the value of just 0.076 dpa. The contribution of a Cu (n,γ)-reaction is even lower. Thus, the contribution from extra sources of internal re-irradiation in first approximation looks very insignificant to result in the ballistic recoil resolution of Al_2O_3.

By the way, it is possible to point to some possible factors causing the reduction of the Al_2O_3 particle size at low irradiation doses.

- The Al_2O_3 crystal has a high oxygen density, which can efficiently scatter from the oxide into the Cu matrix. Following the depletion of oxygen the blankets of Al_2O_3 become unstable and Al can also leave for the Cu matrix.
- Since the matrix has enough B and Li ions that have a high oxygen affinity, the oxygen atom dissipated or diffused from Al_2O_3 will be efficiently bound into

complexes of grain bodies and will now allow the oxygen to revert to Al_2O_3. Part of free oxygen in the matrix will also participate in the nucleation of vacancy pores [41]. Redundant Al will also remain in the matrix in which the solubility at these concentrations is quite sufficient.

- We should point out that it is allowed to transfer properties of large Al_2O_3 specimens on directly properties of microparticles of about 8 nm, but irradiation to 1 dpa of Al_2O_3 shows that this material is not very stable under irradiation [42]. The thermal conductivity and the mechanical properties of Al_2O_3 decrease after irradiation at this comparably low dose.

It is possible to assume that the main reason of changes in the Al_2O_3 particle size under irradiation are the processes of dynamic recoil resolution, Al and O ion scattering from Al_2O_3 and stimulated by irradiation diffusion processes.

5. Conclusions

The performed studies have shown that the GlidCop Al25 IG alloy containing boron in the capacity of deoxidizer is a serious problem due to its resistance to swelling. Even at low doses of about 0.5 dpa it swells at the rate 1%/dpa which is similar to copper. This high swelling rate results from the high helium accumulation rate in the alloy. The MAGT0.2 alloy which does not contain boron (and helium) under the same irradiation conditions does not reveal swelling. The irradiation to 0.5 dpa causes a reduction of the Al_2O_3 particles when they were irradiated at 160 and 300 °C. The assessment of the helium accumulation rate in the GlidCop Al25 IG alloy under fusion relevant conditions means that swelling problems may be created though the rate in fusion reactors is lower but sufficiently high (up to 40 appm/dpa) for alloys containing boron.

References

[1] S.J Zinkle, S.A. Fabritsiev, Atomic and plasma materials interaction data for fusion, J. Nucl. Fusion 5 ((Suppl.)) (1994) 163.
[2] R. Matera, G. Federici, ITER Joint Central Team, J. Nucl. Mater. 233–237 (1996) 17.
[3] G. Kalinin, W. Gauster, R. Matera, A.-A. Tavassoli, A. Rowcliffe, S. Fabritsiev, H. Kawamura, J. Nucl. Mater. 233–237 (1996) 9.
[4] H.R. Brager, H.L. Heinisch, F.A. Garner, J. Nucl. Mater. 133&134 (1985) 676.
[5] H.R. Brager, J. Nucl. Mater. 141–143 (1986) 79.
[6] D.J. Edwards, K.R. Anderson, F.A. Garner, M.L. Hamilton, J.F. Stubbins, A.S. Kumar, J. Nucl. Mater. 191–194 (1992) 416.
[7] K.R. Anderson, F.A. Garner, M.L. Hamilton, J.F. Stubbins, Proceedings of the 15th ASTM International Symposium on the Effect of Radiation on Materials, June 1990, ASTM STP 1125, 1992, p. 854.
[8] S.J. Zinkle, K. Farrel, J. Nucl. Mater. 168 (1989) 262.
[9] M. Ames, G. Kohse, T.S. Lee, N.J. Grant, O.K. Harling, J. Nucl. Mater. 141–143 (1986) 174.
[10] J.A. Spitznagel, N.J. Doyle, W.J. Choyke, J.G. Greggi Jr., J.N. McGruer, J.W. Davis, Nucl. Instrum. and Meth. B 16 (1986) 279.
[11] R.R. Solomon, J.D. Troxell, A.V. Nadkarni, J. Nucl. Mater. 233–237 (1996) 542.
[12] A.S. Pokrovsky, S.A. Fabritsiev, D.J. Edwards, S.J. Zinkle, A.F. Rowcliffe, J. Nucl. Mater. 283–287 (2000) 404.
[13] S.A. Fabritsiev, A.S. Pokrovsky, D.J. Edwards, S.J. Zinkle, A.F. Rowcliffe, J. Nucl. Mater. 283–287 (2000) 523.
[14] S.A. Fabritsiev, A.S. Pokrovsky, D.J. Edwards, S.J. Zinkle, A.F. Rowcliffe, R. Solmon, Plasma Devices Operat. 7 (2001) 31.
[15] S.A. Fabritsiev, A.S. Pokrovsky, D.J. Edwards, S.J. Zinkle, A.F. Rowcliffe, J. Nucl. Mater. 258–263 (1998) 2069.
[16] A.V. Karasiov, S.A. Fabritsiev, J. Nucl. Mater. 233–237 (1996) 1481.
[17] F. Ernst, P. Pirouz, A.H. Heuer, Philos. Mag. A 63 (1991) 259.
[18] B.N. Singh, D.J. Edwards, P. Toft, J. Nucl. Mater. 238 (1996) 244.
[19] D.J. Edwards, F.A. Garner, J.W. Newkirk, A. Nadkarni, J. Nucl. Mater. 212–215 (1994) 1313.
[20] S.J. Zinkle, A. Horsewell, B.N. Singh, W.F. Sommer, J. Nucl. Mater. 195 (1992) 11.
[21] H.R. Brager, J. Nucl. Mater. 141–143 (1986) 163.
[22] S.J. Zinkle, E.V. Nesterova, V.R. Barabash, V.V. Rybin, A.V. Naberenkov, J. Nucl. Mater. 208 (1994) 119.
[23] J.W. Muncie, B.L. Eyre, C.A. English, Philos. Mag. A 52 (1985) 309.
[24] N. Yoshida, Y. Akashi, K. Kitajima, M. Kiritani, J. Nucl. Mater. 133–134 (1985) 385.
[25] S.J. Zinkle, B.N. Singh, J. Nucl. Mater. 283–287 (2000) 306.
[26] N. Wanderka, Y. Yang, L. Jiao, R.P. Wahi, H. Wollenberger, J. Nucl. Mater. 191–194 (1992) 1356.
[27] D.J. Edwards, J.W. Newkirk, F.A. Garner, M.L. Hamilton, A. Nadkarni, Proceedings of the 16th ASTM International Symposium on the Effect of Radiation on Materials, June 1992, ASTM STP 1175, 1994, p.1041.
[28] F.A. Garner, H.R. Brager, K.R. Anderson, J. Nucl. Mater. 179–182 (1991) 250.
[29] S.A. Fabritsiev, S.J. Zinkle, B.N. Singh, J. Nucl. Mater. 233–237 (1996) 127.
[30] H.M. Frost, J.C. Kennedy, J. Nucl. Mater. 141–143 (1986) 169.
[31] S.A. Fabritsiev, A.S. Pokrovsky, S.J. Zinkle, D.J. Edwards, in: Proceedings of 19th International Symposium Effects of Radiation on Materials, Seattle, US, June 1999.
[32] S.J. Zinkle, K. Farrell, H. Kanazawa, J. Nucl. Mater. 168 (1991) 262.
[33] T. Muroga, H. Watanabe, N. Yoshida, H. Kurishita, M.L. Hamilton, J. Nucl. Mater. 225 (1995) 137.

[34] P. Vela, B. Russell, J. Nucl. Mater. 19 (1966) 312.
[35] P. Vela, J. Hardy, B. Russell, J. Nucl. Mater. 26 (1968) 129.
[36] P.J. Maziasz, J. Nucl. Mater. 108–109 (1982) 359.
[37] S.A. Fabritsiev, V.D. Yaroshevich, Strength Mater. 18 (1986) 1194 (Problemy Prochnosti 9 (1986) 48, in Russian).
[38] H. Wollenberger, J. Nucl. Mater. 179–181 (1991) 76.
[39] K.C. Russell, Prog. Mater. Sci. 28 (1984) 229.
[40] L.K. Mansur, K. Farrell, J. Nucl. Mater. 170 (1990) 236.
[41] S.J. Zinkle, Proceedings of the 15th ASTM International Symposium on the Effect of Radiation on Materials, June 1990, ASTM STP 1125, 1994, p. 813.
[42] G.P. Pells, M.J. Murphy, J. Nucl. Mater. 183 (1991) 137.